Journal of the Atmospheric Sciences

A general description of entrainment in buoyant cloudy plumes including the effects of mixing induced evaporation

--Manuscript Draft--

Manuscript Number:	JAS-D-17-0326
Full Title:	A general description of entrainment in buoyant cloudy plumes including the effects of mixing induced evaporation
Article Type:	Article
Corresponding Author:	Julien Savre, Ph.D. Ludwig Maximilian Universität Munich, GERMANY
Corresponding Author's Institution:	Ludwig Maximilian Universität
First Author:	Julien Savre, Ph.D.
Order of Authors:	Julien Savre, Ph.D.
	Michael Herzog, PhD
Abstract:	In this work, the steady-state one-dimensional axisymmetric plume theory is revisited and generalized to include the effects of non homogeneous updraft velocity and buoyancy profiles across the plume, environmental shear and, more importantly, evaporative cooling resulting from the mixing between cloudy air and the dry environment. Based on an energy consistency argument, a method is proposed to derive a relationship for the fractional lateral mixing rate (which may here be positive or negative) from the plume's integral equations, as well as a set of equations for the equivalent plume properties, both of which maintain a high degree of generality by incorporating effects of environmental shear and inhomogeneous radial distributions. In the absence of wind shear, a simpler entrainment rate closure is proposed which is then further constrained by systematically varying the plume and environmental conditions and allowing evaporative cooling to occur. The fractional mixing rate is shown to be strongly correlated with the plume buoyancy and, to a lesser extent, to the critical mixing fraction (i.e. the fraction of dry air that needs to be mixed with cloudy air to make the mixture neutrally buoyant). Quantitative estimates of this dependency are given to facilitate implementations of the new model in convection parameterizations. Analyzing the proposed closure suggests that it could capture features observed in recent high-resolution simulations and that it is consistent with the buoyancy sorting concept. The results therefore support recent findings concerning the parameterization of entrainment for moist atmospheric convection.

"A general description of entrainment in buoyant cloudy plumes including the effects of mixing induced evaporation"

Julien Savre and Michael Herzog

Third round of revisions

The authors would again like to thank reviewer 2 for all his/her valuable comments and suggestions, and overall for all the efforts put in reviewing this manuscript.
The authors would also like to point out that in addition to the (mostly straightforward) corrections made in response to reviewer 2, Figure 5 as well as the text in section 3.d have been modified. A better fit to the data shown on figure 5 and discussed in section 3.d have indeed been found and is now highlighted in the manuscript.

Reviewer #2:

Minor comments:

1. line 17, abstract. "maintaining" should be "maintain".
Corrected.
2. line29. Abstracts are typically not written first or second person. I suggest replacing "Our results" by "The results".
OK, done.
3. line 50. Suggest deleting "As a matter of fact", and replace "efforts" with "effort".
Done.
4. line53. Suggest replacing "high" with "large".
Done.
5. line 79, and elsewhere throughout the paper. I think "gaussian" should be capitalized, i.e. "Gaussian"?
This should indeed be the case and has been corrected in the entire manuscript.
6. line 82. Replace "crossflow" with "sheared flow", based on my point in the previous review that you addressed everywhere else in the paper except here.
We chose here to replace "crossflow" by "sheared environment" to remain consistent with the remainder of the manuscript.
7. line 87. Suggest replacing "precise" with "detailed" - these two words are not synonymous.
Done.
8. line 94. Replace "winds" with "wind".
Done.
9. line 105. Replace "on" with "in".
Done.
10. line 105. I'd suggest simply referring to Table 1 here, rather than the appendix (moreover, there is no appendix 5, I think you meant appendix A). There's no need for an appendix that only refers to one table.
Appendix A has been completely removed, and the table has now been inserted in the main text and is referred to as Table 1.
11. line 108. I feel that the word "exact" should be removed here, since in fact you are not deriving "exact" equations, but are making approximation to the governing equations. This is perhaps a minor quibble, but I feel it should be changed.
"exact" has been removed as suggested.
12. line 112. Add "flux" after "buoyancy".
Corrected.
13. line 115. Remove "are".
Done.
14. line 116. I'd suggest removing "very" here.
Done.
15. line 117. Remove the word horizontal here. The Boussinesq approximation used later neglects both horizontal and vertical variations of density (except where coupled with the buoyancy in the vertical momentum equation).
We now only mention the fact that "the Boussinesq approximation will be introduced later...", without reference to horizontal density variations.

16. line 126. Replace "that" with "those".
Done.
17. line 141. What is "section b"? I think you mean section 2b? Also, you refer to figure 6 here but I believe it's AMS journal policy that figures must be numbered in the order they're cited in papers. Of course, this can be worked out at the technical editing stage once the paper is accepted.
Section 2.b should indeed be referenced here, and this has been corrected. The reference to figure 6 has however been removed.
18. line 170. "latter" is ambiguous here. Are you specifically referring to either Eq. (6) or (7). I think you mean Eq. (6) since pressure does not explicitly appear in that equation.
"latter" refers to equation 7, as the pressure term appears on the left hand side but is dropped on the right hand side. This is specified in the text.
19. line 187. Suggest replacing "introduced" with "used". Also, "external" is confusing here, because this accounts for perturbation pressure which is not necessarily an "external" force to the updraft. Perhaps just replace "external" with "pressure", since the virtual mass parameter does in fact account for buoyant pressure forcing (see, for example, reject papers by Jeevanjee and Romps on this point)?
Both "introduced" and "external" have been replaced as suggested.
20. line 195. I'm not sure what you mean by "suppressing all pressure feedbacks". Maybe replace "suppressing" by "neglecting".
"neglecting" is now used here. Overall, the sentence has also been slightly shortened.
21. line 199. These papers show that the buoyant perturbation pressure field depends directly on the updraft's buoyancy and size, not necessarily on the dynamic pressure field. Thus, replace "dynamical" with "buoyant perturbation". As an aside, I will note that indeed the dynamic perturbation pressure also scales with the updraft buoyancy and size, but the scaling and mechanisms for this are completely different from those described in Markowski and Richardson (2010) and Morrison (2016) for the buoyancy perturbation pressure scaling.
"dynamical" has been replaced by "buoyant perturbation", as suggested.
22. line 210-212. Suggest a rewording here to: "With no direct contribution from pressure forces on scalar fluctuations, even though these fluctuations may exert a strong influence on the plume's development...". Otherwise, this sentence seems to be saying that there is no contribution from pressure forces on updrafts, which is of course not true.
The sentence has been rewritten according to the above suggestion.
23. line 253. I think you should replace "shear less" with unsheared".
Done.
24. line 308. I don't think you really mean "undefined" here. Suggest replacing "undefined" with "general".
This is correct and has been modified accordingly.
25. line 321. Not clear what "This latter" refers to. Consider replacing with "These latter terms...".
"This latter" has here been removed. Instead, the two sentences have been merged to form a single sentence.
26. line 317. Replace "crossflow" with "environmental shear". This is similar to comment 6 above.
Done.
27. line 338. "The presented results..." is confusing. The results presented where? Be specific here.
We agree that this part needs to be reworded. The sentence now reads: "According to equation 32, important biases may be introduced when diagnosing lateral entrainment...".
28. line 349. Replace "this" with "the".
Done.
29. line 371. Remove "reasons".
Done.
30. line 415. Add a comma after "1.5".
Done.
31. line 439. Suggest removing "just below the freezing level". This is obvious since you state the temperature is 274 K.
Done.
32. line 495. I feel you should remove the word "operational" here, since this issue really applies to all convection parameterizations in models, not just those in operational models.
Done.
33. line 499. Replace "this" with "the".

Done.

34. lines 537-538. Replace "elaborated" with "elaborate".

Done.

35. line 594. I'd suggest you remove "however" here, as it's not needed and the sentence flows better without this word.

Done.

36. line 600. Replace "fraction" with "mixing ratio".

Done.

37. line 655. Replace "this" with "the".

Done.

38. line 656. Replace details with detail.

Done.

39. It's not clear what Appendix B is. I'm guessing this was supposed to be removed and wasn't. Also, as noted in comment 10 above, I feel Appendix A should be removed , and you should just refer to Table 1 in the text.

Appendix B was indeed supposed to be removed, and it has now been (no more appendices left).

A general description of entrainment in buoyant cloudy plumes including the effects of mixing induced evaporation

Julien Savre* and Michael Herzog

Department of Geography and Centre for Atmospheric Sciences, University of Cambridge, Downing Place, Cambridge, United Kingdom

*Corresponding author address: Meteorologische Institut, Ludwig-Maximilians Universität, Theresienstr. 37, Munich, Germany

E-mail: julien.savre@lmu.de

ABSTRACT

In this work, the steady-state one-dimensional axisymmetric plume theory is revisited and generalized to include the effects of non homogeneous updraft velocity and buoyancy profiles across the plume, environmental shear and, more importantly, evaporative cooling resulting from the mixing between cloudy air and the dry environment. Based on an energy consistency argument, a method is proposed to derive a relationship for the fractional lateral mixing rate (which may here be positive or negative) from the plume's integral equations, as well as a set of equations for the equivalent plume properties, both of which maintain a high degree of generality by incorporating effects of environmental shear and inhomogeneous radial distributions. In the absence of wind shear, a simpler entrainment rate closure is proposed which is then further constrained by systematically varying the plume and environmental conditions and allowing evaporative cooling to occur. The fractional mixing rate is shown to be strongly correlated with the plume buoyancy and, to a lesser extent, to the critical mixing fraction (i.e. the fraction of dry air that needs to be mixed with cloudy air to make the mixture neutrally buoyant). Quantitative estimates of this dependency are given to facilitate implementations of the new model in convection parameterizations. Analyzing the proposed closure suggests that it could capture features observed in recent high-resolution simulations and that it is consistent with the buoyancy sorting concept. The results therefore support recent findings concerning the parameterization of entrainment for moist atmospheric convection.

1. Introduction

Most present day operational convection parameterizations implemented in numerical weather prediction or climate models rely on the mass flux approach. In such schemes, either the complete cloud spectrum or a single representative bulk cloud must be parameterized to represent the effects of subgrid-scale moist convection, and diagnose the corresponding tropospheric convective heating and moistening. Although important improvements have been made since the pioneering work of (Ooyama 1971), mass flux parameterizations still require *ad-hoc* closures relying on restrictive assumptions. These include 1) a closure relating the intensity of convection to the large-scale atmospheric state, 2) a trigger function to diagnose the onset of convection and 3) a parameterization for the entrainment and detrainment rates quantifying fluxes between clouds and their environment. Parameterizing lateral entrainment is particularly crucial to model the correct vertical distribution of convective mass flux, and therefore that of convective heating and moistening.

In typical mass flux schemes, individual or multiple convective clouds are often represented as one-dimensional buoyant plumes exchanging mass, momentum and energy with their environment (Arakawa and Schubert 1974). The structure of such entraining plumes can be determined by a set of one-dimensional governing equations for either integral (Morton et al. 1956) or primitive (Simpson and Wiggert 1969) quantities, and exchanges of mass and energy between the plumes and their environment are characterized by fractional entrainment/detrainment rates. However, the specification of entrainment/detrainment rates in mass flux schemes relying on the buoyant plume framework remains challenging. Despite much effort since entrainment has been recognized as an important part of the dynamics of rising plumes, proposed entrainment models still lack a sound physical basis, and modelers have to resort to *ad-hoc* relationships derived from high-resolution simulations or intuitive reasoning. As a consequence, the large sensitivity of climate models to the

parameterization of convective entrainment (Klocke et al. 2011; Del Genio 2012) can in part be explained by the fact that important physical processes such as inhomogeneous updraft velocities, evaporative cooling at cloud edges or the presence of environmental shear are often overlooked or too complex to be implemented in simple mass flux schemes.

One important known caveat of most analytical models resides in their inability to account for the mixing between dry and cloudy air and subsequent evaporation. To address this issue, (Raymond and Blyth 1986) proposed the buoyancy sorting concept whereby negatively buoyant air parcels formed after mixing between environmental and cloudy air detrain. This idea was later exploited in various mass flux based convection schemes (Kain and Fritsch 1990; Bretherton et al. 2004). Adopting different approaches, other parameterizations have also been suggested to relate the entrainment rate with environmental conditions, and in particular with relative humidity (Bechtold et al. 2008; Stirling and Stratton 2012). These first attempts to parameterize the effects of mixing and evaporation on entrainment helped to recognize the crucial influence of environmental dryness on the entrainment process. In recent years, more and more modeling studies have therefore focused on the characterization of these effects and on possible ways to connect environmental moisture with entrainment and detrainment (de Rooy and Siebesma 2007; Böing et al. 2012; Dawe and Austin 2013).

In the present study, we chose to adopt an analytical point of view and revisit the one-dimensional steady-state plume theory (Morton et al. 1956; Turner 1986) to derive a general description of convective clouds and lateral entrainment accounting for the effects of cloud edge evaporation. The methodology relies on recent works focusing on buoyant steady-state axisymmetric plumes (Kaminski et al. 2005; van Reeuwijk and Craske 2015), which is here extended to account for environmental wind shear as well as evaporative cooling resulting from the mixing between environmental and cloudy air. The detailed analytical description makes no *a priori*

assumption about the shapes of the radial velocity and buoyancy profiles, although a tentative parameterization of the fractional entrainment rate is proposed after adopting a Gaussian radial distribution for the updraft velocity and assuming that lateral mixing occurs within a linear mixing layer.

In section 2, the extended theory for entraining plumes developing in a sheared environment is exposed and a general entrainment relationship as well as a system of equations describing the plume's vertical structure are derived. The entrainment relationship obtained in the absence of environmental shear is further analyzed in section 3 for non top-hat velocity and buoyancy radial distributions. In particular, the influence of evaporation after mixing between dry and cloudy air is explored to derive a more detailed entrainment rate parameterization as a function of the plume's mean buoyancy. In section 4, the proposed entrainment closure is then compared to various existing models and it is shown that many well accepted results regarding entrainment in convective clouds can be recovered using our analytical description. Our results are finally summarized in section 5.

2. General plume and entrainment theory

a. Governing integral equations

We consider a steady-state buoyant plume rising in the atmosphere in presence of environmental wind. We will assume that the plume is perfectly axisymmetric (with respect to its centerline) although this may not be the case in reality for a plume developing in a sheared environment. Let's define ϕ the angle formed between the centerline of the plume and the horizontal plane. In the tilted plume, we introduce a new curvilinear coordinate system $\{r,s\}$, with s and r the tangential and normal directions with respect to the plume centerline. Let's also define $\boldsymbol{v} = \{v_r, v_s\}$ the

flow velocity relative to the plume in $\{r,s\}$, and $\boldsymbol{u} = \{u,w\}$ the velocity vector expressed in the Cartesian frame. Finally, we define $U_\infty(z) = U_{base} + U_z(z)$ (the subscript ∞ will be used more generally to denote environmental properties), the horizontal component of the environmental flow velocity which we decompose into an invariant part, U_{base}, corresponding to the flow velocity at the base of the plume, and a height dependent component, U_z. The vertical component of the environmental wind is assumed to be zero. A general illustration of the considered geometry is displayed in figure 1. All notations used in this manuscript are summarized in table 1.

In the remainder of this section, we mostly follow methods commonly used to determine the bulk behavior of buoyant plumes and jets in the atmosphere. As such, we are first concerned with deriving equations representing the steady-state distribution of flux quantities with respect to the plume's s-coordinate, integrated over the plume's cross section. In general, such fluxes take the following form:

$$X = 2\int_0^\infty r\widetilde{v_s}x dr,$$

with $x = \{\overline{\rho}, \overline{\rho}\widetilde{v_s}, \overline{\rho}\widetilde{\varphi}, \overline{b'}, \overline{\rho}k\}$ giving $X = \{M,P,S,F,K\}$, where M is the mass flux ($\overline{\rho}$ being the density), P the momentum flux, S the scalar flux ($\widetilde{\varphi}$ representing any given scalar), F the buoyancy flux (with $\overline{b'} = -g(\overline{\rho} - \rho_\infty)$, where $'$ represents a perturbation with respect to the environment) and K is the kinetic energy (k) flux. The density weighted Reynolds average operator $\overline{\rho}\widetilde{\varphi} = \overline{\rho\varphi}$ has been introduced here, where $\overline{\ }$ denotes conventional Reynolds averages and $\widetilde{\ }$ density weighted averages (with their corresponding perturbations $''$). This allows us to keep a general definition of the density in the following derivations (the Boussinesq approximation will be introduced later, in section b).

1) MASS FLUX EQUATIONS

As a starting point, we write the steady-state equation for continuity in the plume's axisymmetric coordinate system. By making the plume fully axisymmetric early in the derivation, we can readily integrate the continuity equation (and, in the following sections, the momentum and scalar equations) over the azimuthal angle. By integration, extra terms arising explicitly from the transformation from the classical equations in Cartesian coordinates to those in the plume's curvilinear coordinates cancel out (these terms involve a partial derivative of the tilt angle with respect to s, see (Schatzmann 1979)).

Using the density weighted averaging operator introduced previously, the continuity equation reads:

$$r\frac{\partial \overline{\rho}\widetilde{v_s}}{\partial s} + \frac{\partial \overline{\rho} r \widetilde{v_r}}{\partial r} = 0,$$

Integrating over the cross direction r between the plume centerline and infinity (therefore considering an isolated plume with well defined constant environmental conditions far enough from the plume center), the mass flux equation becomes:

$$\frac{\partial}{\partial s}\int_0^{+\infty} \overline{\rho} r \widetilde{v_s} dr + [\overline{\rho} r \widetilde{v_r}]_0^{+\infty} = 0. \tag{1}$$

The second term on the left hand side of Equation 1 represents the flux of mass through the plume's boundary which we express following (Hoult et al. 1969):

$$[\overline{\rho} r \widetilde{v_r}]_0^{+\infty} = [\overline{\rho} r (V_e + U_z \sin\phi)]_0^{+\infty} \approx \rho_\infty r_m \left(\alpha_1 v'_{sm} + \alpha_2 |U_z \sin\phi|\right). \tag{2}$$

r_m and v'_{sm} are the top-hat equivalent radius and excess velocity with respect to the background flow along s. Here and in the remainder of this paper, top-hat equivalent quantities correspond to properties that the plume would take if it was finite in size, with radius r_m, and all properties were homogeneous in the radial direction while conserving their total integrals over r. For example for

v'_{sm} we have:

$$\int_0^{+\infty} v'_s(r)\,dr = r_m v'_{sm}$$

This stems directly from the definitions given in section b. The normal velocity $\widetilde{v_r}$ along the plume's boundary has been decomposed into a mean flow contribution $U_z \sin\phi$ and a component V_e representing dynamical entrainment from convergence/divergence normal to the plume. The mean flow contribution only includes the sheared part of the environmental wind, U_z, as the mean background wind, defined at the plume base level, should only advect the plume without contributing to entrainment.

Parameter α_2 appearing on the right hand side of equation 2 quantifies mean flow convergence into the plume. In the case $\alpha_2 = 1$, all the environmental air flowing into the plume accumulates. Advection by the mean wind at all levels without convergence results in $\alpha_2 = 0$. In the remainder of this paper, we will assume $\alpha_2 = 0$, effectively assuming that the background wind does not contribute to lateral entrainment.

Equation 1 can now be written as:

$$\frac{\partial M}{\partial s} = -2\alpha_1 \rho_\infty r_m v'_{sm}, \tag{3}$$

where the integral mass flux in s, M, is defined by:

$$M = 2\int_0^\infty \overline{\rho} r \widetilde{v_s} dr.$$

The fractional mixing rate given by $M^{-1}\frac{\partial M}{\partial s}$ (Simpson and Wiggert 1969), can be obtained directly from equation 3. Although it is common in the literature to distinguish between positive (entrainment) and negative (detrainment) mixing rates (de Rooy et al. 2013), the notation ε, usually referring solely to positive entrainment, will be used in the remainder of this paper to refer to the quantity $M^{-1}\frac{\partial M}{\partial s}$. It follows that: $\varepsilon = -2\alpha_1 \rho_\infty r_m v'_{sm} M^{-1}$.

2) MOMENTUM FLUX EQUATIONS

Equations for the s-momentum $\overline{\rho}\widetilde{v_s}$ and r-momentum $\overline{\rho}\widetilde{v_r}$ can be obtained directly from the steady-state Reynolds averaged equations for the Cartesian horizontal and vertical momentum (ρu and ρw) in the plume's reference frame. From the definition of density weighted Reynolds averages, we have $v_s = \widetilde{v_s} + v_s''$ and $v_r = \widetilde{v_r} + v_r''$, and it follows:

$$\begin{aligned} r\frac{\partial}{\partial s}\overline{\rho}\left(\widetilde{v_s}\widetilde{v_s} + \widetilde{v_s''v_s''}\right) &= -\frac{\partial}{\partial r}\overline{\rho}r\left(\widetilde{v_r}\widetilde{v_s} + \widetilde{v_r''v_s''}\right) - r\frac{\partial p'}{\partial s} - \overline{\rho}r\left(\widetilde{v_s}\widetilde{v_r} + \widetilde{v_s''v_r''}\right)\frac{\partial \phi}{\partial s} + r\overline{b'}\sin\phi \\ r\frac{\partial}{\partial s}\overline{\rho}\left(\widetilde{v_s}\widetilde{v_r} + \widetilde{v_s''v_r''}\right) &= -\frac{\partial}{\partial r}\overline{\rho}r\left(\widetilde{v_r}\widetilde{v_r} + \widetilde{v_r''v_r''}\right) - \frac{\partial r p'}{\partial r} + \overline{\rho}r\left(\widetilde{v_s}\widetilde{v_s} + \widetilde{v_s''v_s''}\right)\frac{\partial \phi}{\partial s} - r\overline{b'}\cos\phi, \end{aligned}$$

with $p' = \overline{p} - p_\infty$ the pressure perturbation (with respect to the environmental state). ϕ was taken to be independent of r, so that $\partial\phi/\partial r = 0$. Assuming that v_r'' fluctuations average out when integrated over the plume's cross section and recognizing that $\widetilde{v_r} = U_\infty \sin\phi$ inside the plume, we can integrate the above equations over r:

$$\frac{\partial}{\partial s}\left[\int_0^{+\infty}\overline{\rho}r\left(\widetilde{v_s}\widetilde{v_s} + \widetilde{v_s''v_s''} + \frac{p'}{\overline{\rho}}\right)dr\right] = \int_0^{+\infty} r\overline{b'}\sin\phi\, dr - U_\infty\sin\phi\frac{\partial\phi}{\partial s}\int_0^{+\infty}\overline{\rho}r\widetilde{v_s}dr - \left[\overline{\rho}r\widetilde{v_r}\widetilde{v_s}\right]_0^{+\infty} \quad (4)$$

$$\frac{\partial}{\partial s}\left(U_\infty\sin\phi\int_0^{+\infty}\overline{\rho}r\widetilde{v_s}dr\right) = -\int_0^{+\infty} r\overline{b'}\cos\phi\, dr + \frac{\partial\phi}{\partial s}\int_0^{+\infty}\rho r\left(\widetilde{v_s}\widetilde{v_s} + \widetilde{v_s''v_s''}\right)dr - \left[\overline{\rho}r\widetilde{v_r}\widetilde{v_r} + rp'\right]_0^{+\infty} \quad (5)$$

Boundary terms representing lateral entrainment into the plume can be expressed following similar arguments as those used in equation 2:

$$\left[\overline{\rho}r\widetilde{v_r}\widetilde{v_s}\right]_0^{+\infty} = -\varepsilon M U_\infty\cos\phi, \quad (6)$$

$$\left[\overline{\rho}r\widetilde{v_r}\widetilde{v_r} + rp'\right]_0^{+\infty} = -\varepsilon M U_\infty\sin\phi. \quad (7)$$

Pressure effects have been neglected on the right-hand side of equation 7 although neglecting all feedbacks between the plume's dynamics and the pressure field may introduce important biases.

Defining the integral $s-$momentum and buoyancy fluxes, denoted P and B respectively:

$$\begin{aligned} P &= 2\int_0^{\infty} \overline{\rho} r \widetilde{v_s}^2 dr \\ B &= 2\int_0^{\infty} r\overline{b'} dr, \end{aligned} \tag{8}$$

equations 4 and 6 (respectively 5 and 7) can then be combined to give:

$$\frac{\partial}{\partial s}\left(\beta P - MU_{\infty}\cos\phi\right) = B\sin\phi - M\cos\phi\frac{\partial U_{\infty}}{\partial s} \tag{9}$$

$$\left(\xi P - MU_{\infty}\cos\phi\right)\frac{\partial\phi}{\partial s} = B\cos\phi + M\sin\phi\frac{\partial U_{\infty}}{\partial s}. \tag{10}$$

Solving equation 9 gives the distribution of the plume's s-momentum (relative to the environmental wind) subject to buoyancy and vertical shear, while equation 10 represents the balance between advection of the plume's angle along s (left hand side), with buoyancy and vertical shear (right hand side). Although we chose to keep the full environmental wind U_{∞} everywhere, only the height dependent term U_z contributes to vertical shear. The complete environmental wind U_{∞} must however be retained in the advective parts of each equation (left hand sides). Under no shear conditions, $\partial\phi/\partial s$ remains equal to zero, and all source terms in equation 10 vanish. The plume cannot develop a tilt and all terms depending on U_{∞} can be omitted as $\cos\phi = 0$. Equation 9 then simply reduces to:

$$\frac{\partial \beta P}{\partial z} = B.$$

In equations 9 and 10, parameters β and ξ account for the bulk effects of turbulent mixing and pressure drag:

$$\begin{aligned} \beta &= 1 + \frac{2}{P}\int_0^{+\infty} \overline{\rho} r \left(\widetilde{v_s'' v_s''} + \frac{p'}{\overline{\rho}}\right) dr \\ \xi &= 1 + \frac{2}{P}\int_0^{+\infty} \overline{\rho} r \widetilde{v_s'' v_s''} dr. \end{aligned}$$

In the atmospheric science literature, a virtual mass parameter, equivalent to $\beta - 1$, is commonly used to account for pressure forces. The virtual mass parameter is typically set to ~ 0.5 (see for

example (Simpson and Wiggert 1969)). Recent high-resolution modeling studies have shown that the dynamical balance inside convective clouds is primarily dominated by buoyancy and pressure gradient forces (de Roode et al. 2012; Romps and Charn 2015). This suggests that $\xi \approx 1$ and $\beta \approx 1.5$, with β only differing from unity because of the pressure contribution (the value $\beta = 1.5$ will be used later in this paper).

A more sophisticated representation of pressure forces would be necessary in order to accurately capture all the interactions between pressure and the plume's dynamics. While our approach effectively neglects all pressure feedbacks, there exists strong numerical and theoretical arguments showing that the plume's and environmental characteristics can actually modulate these forces. In particular, decomposing the perturbation pressure into a dynamical and a buoyant contribution (Morrison 2016), indicates that (1) the buoyant perturbation pressure field depends directly on the updraft's buoyancy and size (Morrison 2016), with larger, more buoyant updrafts having to displace a greater amount of air as they ascend, and (2) vertical wind shear can produce perturbation pressure anomalies affecting the updraft's ascent and geometry (Rotunno and Klemp 1982). Incorporating these effects in our integral plume model is left for future work.

3) SCALAR FLUX EQUATION

We introduce a Reynolds averaged equation for any scalar φ subject to sources and sinks ϖ_φ:

$$r\frac{\partial}{\partial s}\overline{\rho}\left(\widetilde{v_s}\widetilde{\varphi}+\widetilde{v_s''\varphi''}\right)=-\frac{\partial}{\partial r}\overline{\rho}r\left(\widetilde{v_r}\widetilde{\varphi}+\widetilde{v_r''\varphi''}\right)+\overline{\rho}r\widetilde{\varpi_\varphi}.$$

Again, integrating over r with appropriate boundary conditions, and introducing the s-scalar flux S and integrated source term Q_φ:

$$\begin{aligned} S &= 2\int_0^{+\infty}\overline{\rho}r\widetilde{v_s}\widetilde{\varphi}dr \\ Q_\varphi &= 2\int_0^{+\infty}\overline{\rho}r\widetilde{\varpi_\varphi}dr, \end{aligned} \tag{11}$$

one finds:

$$\frac{\partial \kappa S}{\partial s} = \varepsilon M \varphi_\infty + Q_\varphi. \tag{12}$$

Coefficient κ, representing the bulk contribution from scalar turbulent fluxes, is defined by:

$$\kappa = 1 + \frac{2}{S}\int_0^{+\infty} \overline{\rho} r \widetilde{v_s'' \varphi''} dr.$$

With no direct contribution from pressure forces on scalar fluctuations, even though these fluctuations may exert a strong influence on the plume's development, we can hypothesize that κ can take values significantly different from unity (this has however no influence on the entrainment rate formulation discussed in section c).

Based on equation 12, it is easy to derive an equation for the flux of potential temperature, θ. It is then sufficient to replace φ by θ and $\widetilde{\varpi_\varphi}$ by the appropriate sources and sinks of energy (including phase changes and radiation).

4) KINETIC ENERGY FLUX EQUATION

We follow (Kaminski et al. 2005; van Reeuwijk and Craske 2015) and construct an equation for the plume's kinetic energy $k = \widetilde{v_s}\widetilde{v_s} + \widetilde{v_r}\widetilde{v_r}$ by multiplying the s- and r-momentum equations by $2\widetilde{v_s}$ and $2\widetilde{v_r}$ respectively. After lengthy manipulations, one finds the following unapproximated equation:

$$\begin{aligned}
& r\frac{\partial}{\partial s}\left[\overline{\rho}\widetilde{v_s}\left(k + 2\widetilde{v_s''v_s''} + 2\frac{p'}{\overline{\rho}}\right) + 2\overline{\rho}\widetilde{v_r}\widetilde{v_r''v_s''}\right] + \frac{\partial}{\partial r}\left[\overline{\rho} r \widetilde{v_r}\left(k + 2\widetilde{v_r''v_r''} + 2\frac{p'}{\overline{\rho}}\right) + 2\overline{\rho} r \widetilde{v_s}\widetilde{v_r''v_s''}\right] \\
= \; & -2\overline{\rho} r\left(\widetilde{v_s''v_s''}\frac{\partial \widetilde{v_s}}{\partial s} + \widetilde{v_r''v_r''}\frac{\partial \widetilde{v_r}}{\partial r}\right) - 2\overline{\rho} r\left(\widetilde{v_s''v_r''}\frac{\partial \widetilde{v_r}}{\partial s} + \widetilde{v_s''v_r''}\frac{\partial \widetilde{v_s}}{\partial r}\right) - 2rp'\left(\frac{\partial \widetilde{v_s}}{\partial s} + \frac{\partial \widetilde{v_r}}{\partial r}\right) \\
+ \; & 2r\overline{b'}\left(\widetilde{v_s}\sin\phi - \widetilde{v_r}\cos\phi\right) + 2\overline{\rho} r\left(\widetilde{v_r}\widetilde{v_s''v_s''} - \widetilde{v_s}\widetilde{v_s''v_r''}\right)\frac{\partial \phi}{\partial s}.
\end{aligned}$$

The two terms on the left hand side of the above equation are associated with the transport of kinetic energy by the mean wind, where contributions from the mean energy and turbulent fluctuations are represented. The first two terms on the right hand side are generally positive and

represent the production of turbulent kinetic energy by wind shear, while the third term on the right is a pressure redistribution term. The last two terms finally represent the production of kinetic energy by buoyancy and the sink of kinetic energy due to the plume's tilt respectively. After integrating over r with the following boundary condition:

$$\left[\overline{\rho} r \widetilde{v_r}\left(k + 2\frac{p'}{\overline{\rho}}\right)\right]_0^{+\infty} = -\varepsilon M k_\infty = -\varepsilon M U_\infty^2$$

and neglecting terms including fluctuations v_r'' as well as $\partial \widetilde{v_r}/\partial r$ (i.e. the cross velocity v_r is homogeneous across the plume), one finally finds an equation for the integral kinetic energy flux

$$K = 2\int_0^{+\infty} \overline{\rho} r \widetilde{v_s} k dr,$$

as:

$$\frac{\partial \gamma K}{\partial s} = \zeta \rho_\infty r_m v_{sm}'^3 + \varepsilon M U_\infty^2 + 2F\sin\phi - 2BU_\infty \cos\phi \sin\phi \tag{13}$$

where v_{sm} is the top-hat equivalent updraft velocity defined in section b. In equation 13, we have introduced the following integral parameters:

$$\begin{aligned}
\gamma &= 1 + \frac{4}{K}\int_0^{+\infty} \overline{\rho} r \widetilde{v_s}\left(\frac{p'}{\overline{\rho}} + \widetilde{v_s'' v_s''}\right) dr, \\
\zeta &= \frac{4}{\rho_\infty r_m v_{sm}'^3}\int_0^{+\infty} \overline{\rho} r \left(\frac{p'}{\overline{\rho}} + \overline{\rho}\widetilde{v_s'' v_s''}\right)\frac{\partial \widetilde{v_s}}{\partial s} + \overline{\rho} r \widetilde{v_r}\widetilde{v_s'' v_s''}\frac{\partial \phi}{\partial s} dr,
\end{aligned}$$

as well as the buoyancy flux:

$$F = 2\int_0^{+\infty} r \widetilde{v_s}\overline{b'} dr.$$

Coefficient γ is a correction term covering the effects of pressure drag and turbulent fluctuations (similar to β or κ). γ can alternatively be understood as the ratio between the exact kinetic energy flux and its top-hat equivalent counterpart (a similar interpretation can be provided for β). We have gathered all other terms related to kinetic energy production by turbulent fluctuations and shear in ζ. In a non sheared environmental, all terms depending on U_∞ vanish except the entrainment

contribution $\varepsilon M U_\infty^2$, and equation 13 reduces to

$$\frac{\partial \gamma K}{\partial s} = \zeta \rho_\infty r_m v_{sm}'^3 + 2F + \varepsilon M U_\infty^2.$$

b. General velocity and scalar profiles

So far, no assumptions on the radial velocity and thermodynamic profiles have been made. We account for inhomogeneous distributions across the plume by introducing the following shape functions:

$$\begin{aligned}
\overline{b'}(r,s) &= b'_m(s)\, e(r), \\
\widetilde{v_s}(r,s) &= U_\infty \cos\phi + v'_{sm}(s)\, f(r), \\
\widetilde{\varphi}(r,s) &= \varphi_\infty(s) + \varphi'_m(s)\, g(r),
\end{aligned}$$

All perturbations with respect to environmental values have been expressed as the product of top-hat equivalent quantities varying in s only (subscripts m) and the normalized radial distributions e, f and g. For simplicity, we also set $\overline{\rho} = \rho_\infty$ following the Boussinesq approximations. Let's now introduce the following shape integrals:

$$I_1 = \frac{2}{r_m^2}\int_0^{+\infty} r f(r)\, dr, \tag{14}$$

$$I_2 = \frac{2}{r_m^2}\int_0^{+\infty} r e(r)\, dr, \tag{15}$$

$$I_3 = \frac{2}{r_m^2}\int_0^{+\infty} r e(r) f(r)\, dr, \tag{16}$$

$$I_4 = \frac{2}{r_m^2}\int_0^{+\infty} r f^2(r)\, dr, \tag{17}$$

$$I_5 = \frac{2}{r_m^2}\int_0^{+\infty} r f^3(r)\, dr, \tag{18}$$

$$I_6 = \frac{2}{r_m^2}\int_0^{+\infty} r g(r)\, dr, \tag{19}$$

$$I_7 = \frac{2}{r_m^2}\int_0^{+\infty} r g(r) f(r)\, dr. \tag{20}$$

By definition, we have: $I_1 = I_2 = I_6 = 1$. Making use of the above definition of $\widetilde{v_s}$ with $I_1 = 1$, the mass flux M can be rewritten as:

$$M = 2\int_0^{+\infty} \overline{\rho} r \widetilde{v_s} dr = \rho_\infty r_m^2 v'_{sm} \left(1 + \frac{U_\infty}{v'_{sm}} \cos\phi\right) = \rho_\infty r_m^2 v'_{sm} J_1.$$

where we have set $J_1 = 1 + \frac{U_\infty}{v'_{sm}} \cos\phi$. Using a similar reasoning, the s-momentum, scalar and kinetic energy fluxes can be expressed as:

$$\begin{aligned} P &= \rho_\infty r_m^2 v'^2_{sm} J_4 + M U_\infty \cos\phi, \\ S &= \rho_\infty r_m^2 v'_{sm} \varphi'_m J_7 + M \varphi_\infty, \\ K &= \rho_\infty r_m^2 v'^3_{sm} J_5 + 2\rho_\infty r_m^2 v'^2_{sm} U_\infty \cos\phi J_4 + M U_\infty^2, \end{aligned} \tag{21}$$

with $J_4 = I_4 + \frac{U_\infty}{v'_{sm}} \cos\phi$, $J_7 = I_7 + \frac{U_\infty}{v'_{sm}} \cos\phi$, and $J_5 = I_5 + I_4 \frac{U_\infty}{v'_{sm}} \cos\phi$. Note that in an unsheared environmental flow, we have $J_1 = I_1 = 1$, $J_4 = I_4$, $J_5 = I_5$ and $J_7 = I_7$.

Using the above expressions for mass, momentum and scalar fluxes, we can now define the top-hat variables r_m, v'_{sm}, and φ'_m as functions of integral fluxes and shape integrals only:

$$r_m = \sqrt{\frac{J_4}{\rho_\infty (P - M U_\infty \cos\phi)}} \frac{M}{J_1}, \tag{22}$$

$$v'_{sm} = \frac{P - M U_\infty \cos\phi}{M} \frac{J_1}{J_4}, \tag{23}$$

$$\varphi'_m = \frac{S - M\varphi_\infty}{M} \frac{J_1}{J_7}. \tag{24}$$

c. Entrainment rate closure

Using 22 and 23, the plume kinetic energy can be recast into the following form:

$$K = M U_\infty^2 + (P - M U_\infty \cos\phi) \left[\frac{J_5 J_1}{J_4^2} \frac{P}{M} + \left(2 - \frac{J_5 J_1}{J_4^2}\right) U_\infty \cos\phi\right]. \tag{25}$$

By differentiating 25 with respect to s, equating with equation 13 and further assuming full self-similarity (turbulence in the plume is fully developed so that all shape parameters are assumed to

be independent on the plume's coordinate s (van Reeuwijk and Craske 2015)), a closed form of the fractional entrainment rate parameter ε can be found. The entrainment parameter thus obtained is energy consistent, i.e. it balances exactly the production of integral kinetic energy within the plume (equation 13) with the transport of integral momentum based on equation 9.

When environmental shear is explicitly considered, the analytical form of the entrainment rate parameter ε obtained (not shown) includes contributions from the environmental wind shear and plume tilt. However, its complexity and the introduction of many unclosed parameters makes it difficult to employ in practice. Although we can only speculate that environmental shear will affect the entrainment process, a no shear situation will be considered in the following, with U_∞ independent of height and $\phi = \frac{\pi}{2}$. The entrainment relationship now reduces exactly to:

$$\varepsilon r_m = -\frac{\zeta}{\gamma^*} + 2\left(\frac{1}{\beta^*} - \frac{\sigma}{\gamma^*}\right) Ri. \tag{26}$$

$Ri = r_m b'_m / \left(\rho_\infty w_m^2\right)$ is a convective Richardson number, and the following modified parameters have been introduced:

$$\begin{aligned} \gamma^* &= \gamma J_5 \\ \beta^* &= \beta J_4. \\ \sigma &= I_3. \end{aligned}$$

σ quantifies the mismatch between the buoyancy and updraft velocity profiles and indicates how similar (different) both distributions are ($\sigma = 1$ corresponding to identical distributions). In equation 26, the fractional entrainment rate ε is expressed as the sum of two terms: the first one includes contributions from turbulent fluctuations and pressure drag while the second one quantifies the competition between buoyancy and inertia through Ri, thus giving a measure of how forced the plume is (small Ri indicating highly forced plumes with behaviors similar to pure jets). Ri is itself corrected by a factor accounting for turbulent fluctuations, pressure forces and the mismatch

parameter σ. Equation 26 is consistent with previously published relationships (Fox 1970; Schatzmann 1979; Kaminski et al. 2005; van Reeuwijk and Craske 2015) derived under dry conditions.

Assuming that all quantities are characterized by top-hat radial distributions across the plume, all shape integrals I_1 through I_7 are equal to unity (this also implies that: $J_1 = J_4 = J_5 = 1$). The modified parameters in equation 26 can thus be replaced by their uncorrected equivalents β and γ. Taking one step further and letting $\beta = \gamma$ in 26, that is assuming that both the *s*-momentum and in-plume kinetic energy fluxes are not affected by turbulent fluctuations and pressure drag, yields a classical form of the fractional entrainment rate whereby $\varepsilon \propto r_m^{-1}$. Such a formulation suffers however from obvious deficiencies: all quantities are crudely assumed to be perfectly homogeneous inside the plume, entrained air is instantaneously homogenized within the plume, ε is necessarily positive and therefore does not allow detrainment (detrainment must then be arbitrarily parameterized, for example, at the level of neutral buoyancy), and ε does not depend on any dynamical or thermodynamical properties of the plume or the environment.

In the more general case, *Ri* can be positive or negative reflecting the possibility for plume air to detrain. In particular, setting $\sigma = 1$ and thereby assuming that the in-plume distributions of updraft velocity and buoyancy match perfectly (in other words, $e(r) = f(r)$), negative buoyancy is likely to imply detrainment provided that $2\left(\frac{1}{\beta^*} - \frac{1}{\gamma^*}\right) Ri < \left|\frac{\zeta}{\gamma^*}\right|$. If, for example, a slowly rising plume (low updraft velocities) overshoots its level of neutral buoyancy and becomes negatively buoyant (i.e. large negative *Ri*), the resulting large negative ε values would be associated with the formation a layer of strong detrainment capping the plume. However, if the plume becomes negatively buoyant but maintains large updraft velocities, positive entrainment may still result, and the plume may not necessarily die out.

As will be demonstrated in section 3, accounting for more realistic distributions of vertical velocity and buoyancy, i.e. allowing $\sigma \neq 1$, can substantially affect the entrainment process and notably account for the influence of environmental relative humidity.

d. Equations for top-hat variables

Using the general flux equations derived previously we can arrive at a system of equations for the primitive top-hat variables characterizing the plume. The proposed system still maintains all its generality and includes both the effects of environmental wind and general radial distributions. By combining equations 3, 9, 10 and 12 with the definitions of top-hat quantities, we obtain:

$$\frac{2}{r_m}\frac{\partial r_m}{\partial s} = J_1\left(\varepsilon - \frac{1}{v'_{sm}}\frac{\partial v'_{sm}}{\partial s} - \frac{1}{g}N_\infty^2\right), \tag{27}$$

$$\frac{\partial v'_{sm}}{\partial s} = -\varepsilon v'_{sm}\left[1 + \frac{J_1}{J_4}\left(1 - \frac{1}{\beta}\right)\frac{U_\infty}{v'_{sm}}\cos\phi\right] + \frac{1}{\beta^*}\frac{b'_m}{\rho_\infty v'_{sm}}\sin\phi \tag{28}$$

$$+ \frac{J_1}{J_4}\left(1 - \frac{1}{\beta}\right)U_\infty \sin\phi\frac{\partial\phi}{\partial s} - \frac{J_1}{J_4}\cos\phi\frac{\partial U_\infty}{\partial s}, \tag{29}$$

$$\frac{\partial\phi}{\partial s} = \frac{\frac{b'_m}{\rho_\infty v'_{sm}}\cos\phi + J_1\frac{\partial U_\infty}{\partial s}\sin\phi}{\xi^* v'_{sm}\left[1 + \frac{J_1}{J_4}\left(1 - \frac{1}{\xi}\right)\frac{U_\infty}{v'_{sm}}\cos\phi\right]} \tag{30}$$

$$\frac{\partial\varphi'_m}{\partial s} = \varepsilon\left[\frac{J_1}{J_7}\left(\frac{1}{\kappa} - 1\right)\varphi_\infty - \varphi'_m\right] + \frac{Q_\varphi}{\kappa^* v'_{sm}} - \frac{J_1}{J_7}\frac{\partial\varphi_\infty}{\partial s}, \tag{31}$$

Where we have introduced the buoyancy frequency with respect to the plume's coordinate system: $N_\infty^2 = 1/\rho_\infty\,(\partial\rho_\infty/\partial s)$, the top-hat equivalent buoyancy b'_m (which can be positive or negative), and the modified parameter $\xi^* = \xi J_4$.

Under no shear conditions, that is if U_∞ is homogeneous and independent of height, $\cos\phi$ remains equal to zero as the plume is unable to develop any tilt (see section 2), all terms depending explicitly on U_∞ vanish, and the updraft velocity equation reduces to a more typical form where only two terms remain on the right hand side, entrainment and buoyancy:

$$\frac{\partial w_m}{\partial z} = -\varepsilon w_m + \frac{1}{\beta^*}\frac{b'_m}{\rho_\infty w_m}.$$

Similarly, in the absence of a sheared environment, and considering a passive tracer ($Q_\varphi = 0$), the equation for $\varphi_m = \varphi_\infty + \varphi'_m$ becomes:

$$\frac{\partial \varphi_m}{\partial z} = \varepsilon \left(\varphi_\infty - \varphi_m\right) + \left(1 - \frac{1}{I_7}\right) \frac{\partial \varphi_\infty}{\partial z} + \varepsilon \frac{1}{I_7} \left(\frac{1}{\kappa} - 1\right) \varphi_\infty. \tag{32}$$

This equation is similar to that typically used to diagnose entrainment from high-resolution model output (de Rooy et al. 2013), except for the last two terms on the right hand side which depend directly on the ratio $1/I_7$ representing, like σ, the mismatch between the updraft velocity and scalar profiles across the plume. To recover a more classical form of the scalar equation, κ must first be set to unity, i.e. the effects of turbulent fluxes $\widetilde{v''_s \varphi''}$ integrated over the plume's cross section must be neglected (see section 3). We can however expect these fluxes to be important for the plume's evolution, in particular when considering how humidity fluctuations in the atmosphere can affect a cloud's microphysical properties and its vertical extent. If we describe both radial distributions of updraft velocity and passive tracer by Gaussian functions (see equation 33) of different widths, we find $I_7 = 2/\left[\left(\frac{r_m}{r_m+\Delta}\right)^2 + 1\right]$, where r_m is the top-hat radius and Δ is the radius difference between the velocity and scalar profiles. For $\Delta = 0$, that is if the scalar and updraft velocity distributions are similar, $I_7 = 1$ and equation 32 reduces to its typical simplified form where only the first term on the right hand side remains (a similar situation is found when the updraft velocity and passive tracer assume top-hat distributions). For $\Delta > 0$, that is if the scalar anomaly extends beyond the plume core limits, we have $I_7 > 1$ and $\left(1 - \frac{1}{I_7}\right) \frac{\partial \varphi_\infty}{\partial z}$ can no longer be ignored. In particular, considering a scalar for which $\partial \varphi_\infty / \partial z < 0$ (e.g. the total water q_t in the atmosphere), the term $\left(1 - \frac{1}{I_7}\right) \frac{\partial \varphi_\infty}{\partial z} < 0$ provides a sink of ϕ_m. Similarly, considering a scalar for which $\partial \varphi_\infty / \partial z > 0$ (e.g. the liquid potential temperature θ_l), $\left(1 - \frac{1}{I_7}\right) \frac{\partial \varphi_\infty}{\partial z} > 0$ provides a source of ϕ_m.

According to equation 32, important biases may be introduced when diagnosing lateral entrainment in high-resolution simulations when only $\varepsilon \left(\varphi_\infty - \varphi_m\right)$ is considered on the right-hand side.

In particular, errors related to turbulent fluxes of the considered scalar through the plume as well as the mismatch between the updraft velocity and buoyancy radial profiles (presence of a cloud shell) should be accounted for explicitly.These biases could also explain why the use of different conserved scalars (q_t or θ_l) often yields different bulk entrainment estimates, and why entrainment diagnosed directly from high-resolution simulations differ so much from bulk entrainment rates (Romps 2010; Dawe and Austin 2011).

3. Varying velocity and buoyancy radial distributions

We explore here the influence of realistic velocity and buoyancy radial distributions (the latter being affected by phase changes resulting from the mixing of moist and dry air parcels) on the fractional entrainment rate given by equation 26. In the remainder, we will only consider buoyant plumes developing in a non sheared environment with U_∞ independent of height, and $\phi = \frac{\pi}{2}$ ($\cos\phi = 0$). As a consequence, notations in Cartesian coordinates will be employed, such that $s \rightarrow z$ and $v_s \rightarrow w$.

a. Complex velocity and buoyancy profiles

We now postulate that the velocity assumes the following Gaussian radial distribution (Turner 1986; van Reeuwijk and Craske 2015):

$$\widetilde{w}(r,z) = 2w_m(z)\exp\left(-2\frac{r^2}{r_m^2}\right). \tag{33}$$

We also define the in-plume buoyancy distribution based on a mixing fraction χ varying between 0 in the environment and 1 in the plume core, and representing the fraction of environmental air mixed within the plume. It is assumed to depend only on the position r within a mixing layer of specified width λ, located between $r_m(1-\lambda/2) < r < r_m(1+\lambda/2)$, and centered around $\chi(r_m) = 0.5$ (see figure 6). λ has been normalized so that it varies between 0 (no mixing at all)

and 2 (environmental air mixed all the way to the plume's centerline). Although we acknowledge that λ constitutes a crucial parameter controlling cloud dilution, its precise characterization is left for future work. We can only speculate here that λ depends strongly on the competition between turbulent mixing at cloud edge and cloud droplet evaporation. Thermodynamic properties are held equal to their plume or environmental values outside of this layer. We follow (Raymond and Blyth 1986) and (Bretherton et al. 2004) and define the mixing fraction χ as a linear function of the radius r within the mixing layer:

$$\chi = \min\left(\max\left(0.5 - \frac{1}{\lambda}\left(1 - \frac{r}{r_m}\right);0\right);1\right). \tag{34}$$

All thermodynamic variables are then assumed to follow uniform distributions within the mixing layer, so that all mixing states have equal probabilities to occur (Bretherton et al. 2004).

For simplicity, both the updraft velocity and buoyancy radial distributions are supposed to remain independent of height, that is their shapes are preserved when rescaled by the plume's radius at any given altitude (full self-similarity, which also implies that parameters β, σ or ζ are also independent of altitude). This latter assumption may be violated close to the plume source as plume edge turbulence may require time to fully develop.

Thermodynamic and water properties are computed explicitly as functions of χ following (Korolev et al. 2016). The properties estimated are the temperature T, relative humidity RH, water vapor mixing ratio q_v, and cloud liquid mixing ratio q_l. Boundary conditions are taken in the far-field environment and at the center of the cloud (subscripts c below). In practice, the temperature and moisture content of mixed parcels are first calculated before any phase changes occur. Introducing the symbols $\langle . \rangle_0$ and $\langle . \rangle$ to denote mixture properties before and after phase changes, the

vapor and liquid mixing ratios before evaporation are given by:

$$\langle q_v \rangle_0 = \chi q_{v\infty} + (1-\chi) q_{vc}, \tag{35}$$

$$\langle q_l \rangle_0 = (1-\chi) q_{lc}, \tag{36}$$

Energy conservation imposes that the temperature in the mixed parcel before evaporation is given by:

$$\langle T \rangle_0 = \frac{\alpha\chi T_\infty + (1-\chi) T_c}{\alpha\chi + (1-\chi)} \tag{37}$$

with:

$$\alpha = \frac{1 + \frac{c_{pv}}{c_{pa}} q_{s\infty}}{1 + \frac{c_{pv}}{c_{pa}} q_{sc}}. \tag{38}$$

q_s is the saturation vapor mixing ratio, c_{pv} and c_{pa} are the heat capacities at constant pressure for water vapor and dry air. To a good approximation, $\alpha \sim 1$. Once the mixing state before evaporation is obtained, the amount of vapor required to saturate the parcel is computed using the Clausius-Clapeyron relationship, yielding:

$$\delta q_v = -a \log\left(\frac{1 + b\langle RH \rangle_0}{1+b}\right), \tag{39}$$

with

$$b = \frac{e_s R_a L_v^2}{p c_{pa} R_v^2 \langle T \rangle_0^2} \qquad a = \frac{c_{pa} R_v \langle T \rangle_0^2}{L_v^2}. \tag{40}$$

R_v and R_a are the specific gas constants for water vapor and dry air respectively, e_s is the saturation vapor pressure, p the atmospheric pressure, and L_v the latent heat of vaporization. If $\delta q_v > \langle q_v \rangle_0$, all the liquid evaporates so that $\langle q_l \rangle = 0$ and $\langle q_v \rangle = \langle q_v \rangle_0 + \langle q_l \rangle_0$. However, if some liquid remains, then $\langle q_l \rangle = \langle q_l \rangle_0 - \delta q_v$ and $\langle q_v \rangle = \langle q_v \rangle_0 + \delta q_v$. In any case, the parcel temperature is obtained using $\langle T \rangle = \langle T \rangle_0 - \frac{L_v}{c_{pa}} \delta q_v$. The density, and therefore the buoyancy in the mixed parcel, are retrieved using the ideal gas law applied to moist air: $p = \rho \left(1 + \frac{R_v}{R_a} q_v\right) R_a T$. After mixing, gradients of q_l, q_v and T are produced within the mixing layer while these quantities remain homogeneous

inside the cloud core and in the environment. Although their respective in-cloud radial distributions may play an important role on the mixture's properties, we chose here to ignore them and focus on the feedbacks between the buoyancy and updraft velocity distributions.

As evaporation is explicitly treated, negatively buoyant mixed air parcels can be produced. A critical value of the mixing fraction, χ_{cr}, is defined when this occurs, such that $b'_m > 0$ for $\chi < \chi_{cr}$ and $b'_m < 0$ for $\chi > \chi_{cr}$. In realistic conditions, χ_{cr} is expected to vary between 1, i.e. cloudy air always remains positively buoyant even after mixing, and values on the order of 0.1 as seen for example in (Böing et al. 2012).

b. No evaporation case

We first consider the example of an entraining dry plume for which both the environmental and plume vapor mixing ratios are set to zero. Considering a Gaussian velocity distribution across the plume according to 33, most shape integrals can be evaluated analytically: $I_1 = I_2 = I_4 = 1$ and $I_5 = 4/3$. $\sigma = I_3$ remains *a priori* unknown and must be solved numerically. Besides, relying on recent experimental studies and high resolution numerical simulations, (van Reeuwijk and Craske 2015) showed that ζ remains close to the widely accepted value of -0.2, whether one considers forced plumes or pure jets. As a result, buoyancy will primarily affect lateral mixing through Ri, thereby suggesting that buoyancy generated turbulence has only a secondary effect on entrainment. Taking to first approximation $\gamma = \beta = 1.5$, the only remaining unknown parameter in Equation 26 is now σ.

As σ can be interpreted as a coupling parameter between the normalized updraft velocity and buoyancy distributions, it remains mostly insensitive to plume core properties. However, as we are using Gaussian updraft velocity and linear buoyancy distributions, σ is found to depend primarily on the mixing layer thickness λ, and varies between 0.864 for a top-hat buoyancy profile ($\lambda = 0$)

and 0.51 for $\lambda = 2$. Note that choosing a Gaussian buoyancy distribution similar to the velocity one gives $\sigma = 1$.

In the absence of plume edge evaporation, we can rewrite 26 as:

$$\varepsilon \approx \frac{1}{r_m}(0.1 + \eta Ri)\,. \tag{41}$$

with:

$$\eta = 1.333 \times (1 - 0.75\sigma)\,. \tag{42}$$

With the limit values under dry conditions $0.51 < \sigma_{dry} < 0.864$, we find $0.47 < \eta_{dry} < 0.82$ (the lower and upper limits correspond to a top-hat buoyancy profile and a fully mixed plume respectively). These values are in good agreement with those found in the literature for dry buoyant plumes and jets with general radial velocity distributions (0.5 in (Chiang and Sill 1985); 0.475 in (List and Imberger 1973); 0.4775 at low *Ri* numbers in (Schatzmann 1979), all close to the top-hat buoyancy limit).

c. Influence of mixing induced evaporation

In the general case, mixing of dry air in the cloudy plume and subsequent condensation/evaporation are expected to affect the radial buoyancy distribution. In order to quantify these effects, we run a number of simple tests following the procedure described previously, varying systematically the cloud and environmental conditions to span a wide range of realistic situations. To be more specific, q_l is varied between 0.1 g/kg and 2 g/kg (representative of shallow non-precipitating, and deep precipitating clouds respectively), RH_∞ is varied between 40% and 99% and the temperature excess within the plume between 0.2 K and 3 K. All the tests use a fixed atmospheric pressure of 700 hPa and in-cloud temperature of 274 K.

Under the Boussinesq approximation, I_4 and I_5 (and thus γ^*) are insensitive to condensation/evaporation and remain equal to 1 and $4/3$ respectively. In contrast, figure 2 shows a strong dependence of σ on the plume's top-hat buoyancy b'_m. Two different mixing layers are displayed, $\lambda = 0.5$ and $\lambda = 2$, although the latter case is expected to represent an unrealistic mixing situation as it would imply that environmental air is able to dilute the entire cloud core at any vertical level (a situation contradicted by LES results showing a progressive erosion of the cloud core, see for example (Romps and Kuang 2010)). No clear correlation was found between σ and first order properties such as the environmental relative humidity (not shown). According to figure 2, σ varies roughly as a hyperbolic function of b'_m, with $\sigma = \sigma_{dry}$ for large values of b'_m. This suggests that if the plume core remains positively buoyant under any mixing condition, cloud edge evaporation does not affect entrainment.

Figure 3 shows the fractional entrainment rate ε as a function of b'_m, for two updraft velocities (0.5 m/s and 2 m/s) and two mixing layer thicknesses. A fixed plume radius of 1000 m was selected here. It appears first that the magnitude of ε is primarily controlled by the updraft velocity through its dependency on Ri. When w_m is increased, the magnitude of the fractional entrainment/detrainment rate is dramatically reduced, consistent with the fact that a slower updraft will have more time to experience dilution when moving over a certain distance compared to a faster updraft. ε also correlates particularly well with b'_m and the environmental relative humidity RH_∞, ε increasing monotonically with both b'_m and RH_∞. The sensitivity of the entrainment rate on these two quantities is however substantially reduced in the higher updraft velocity case.

For a given relative humidity, ε depends linearly on the top-hat buoyancy. When the plume becomes neutrally or negatively buoyant, ε tends to be negative and detrainment occurs. At fixed b'_m, when the environmental relative humidity is increased, ε shifts to higher values by a factor that seems to depend only on w_m and λ. Detrainment thus appears to be favored by both weakly

buoyant clouds and dry environments. Based on these results, we can already infer a functional dependence of ε on b'_m of the form: $\varepsilon \propto xb'_m + yRH_\infty$, with x and y two free parameters depending essentially on w_m and λ.

In addition to the environmental humidity, the entrainment rate is also affected by the cloud liquid mixing ratio. This is particularly true for slow and weakly buoyant plumes in dry environments. Under such conditions, increasing q_l consistently results in lower entrainment (and stronger detrainment) rates. In contrast, when the environment approaches saturation and b'_m is increased, the entrainment rate becomes largely insensitive to q_l. Where q_l has a noticeable impact on entrainment, a plume with a higher liquid water content is found to be more likely to detrain than a plume containing less condensate. This is because a cloud with a higher q_l can potentially evaporate more than a less humid plume, especially in a drier atmosphere, and the stronger evaporative cooling can produce more negatively buoyant parcels.

The mixing layer thickness λ influences both the magnitude and sign of the fractional entrainment rate: thinner mixing layers entrain less and are also less likely to detrain (at $w_m = 0.5$, detrainment occurs below $b'_m \approx 0.05$ for $\lambda = 2$, but below $b'_m \approx 0.025$ for $\lambda = 0.5$). When λ is decreased, the sensitivity of ε to q_l is also reduced but remains nonetheless significant at low b'_m.

Finally, figure 4 displays the fractional entrainment rate ε as a function of the critical mixing fraction χ_{cr}, again for two updraft velocities but with $\lambda = 0.5$ only. Owing to the strong relationship between χ_{cr} and b'_m, ε also correlates well with the critical mixing fraction. In particular, when χ_{cr} becomes small enough, ε becomes negative and detrainment occurs, consistent with the buoyancy sorting concept (Raymond and Blyth 1986). The existence of a direct relationship between ε and χ_{cr} is now less trivial as χ_{cr} appears to be a non-linear function of both the buoyancy and relative humidity (see for example (de Rooy and Siebesma 2007)). Note that the possibility

to parameterize the entrainment rate as a function of χ_{cr} has been previously suggested based on cloud resolving simulation results (de Rooy and Siebesma 2007; Böing et al. 2012).

Overall, the above analysis reveals a complex dependency of the fractional entrainment rate on updraft velocity, buoyancy and relative humidity. In practical applications, additional complications may stem from the fact that all these variables are in fact interdependent, while each variable has here been varied independently. In particular, the updraft velocity depends strongly on buoyancy which is itself affected by relative humidity (and other factors such as temperature). Care should therefore be taken if the present entrainment rate closure is to be implemented in convection parameterizations where such interdependencies are particularly relevant.

d. Tentative entrainment parameterization

The entrainment relationship 26 is now rewritten as follows:

$$\varepsilon = \frac{0.1}{r_m} + \eta \frac{b_m}{\rho_\infty w_m^2}. \tag{43}$$

The first term on the right hand side corresponds to the inverse plume radius dependency used for example by (Simpson and Wiggert 1969), with a constant of proportionality $\zeta/\gamma^* = 0.1$ (half the typical value of 0.2 due to the combined effects of pressure forces and the Gaussian updraft velocity profile). It should be noted however that there is no indication that γ should be similar to β and that β is constant. In the limit that r_m^{-1} is small compared to $Ri = r_m b'^m/\rho_\infty w_m^2$, these assumption are not expected to significantly effect our main conclusions so that η can be chosen to depend solely on σ. As suggested by Figure 5 for the case $\lambda = 0.5$, η (like σ) can be approximated by a hyperbolic function of b'_m tending asymptotically to the dry limit at $\chi_{cr} = 1$. In particular, η seems to be well approximated by a power law function of b'_m:

$$\eta = \eta_0(\lambda) + a b_m'^b. \tag{44}$$

The subscript 0 denotes the asymptotic value of η (dry limit) depending on the mixing layer thickness only. a and b are tunable parameters.

Figures 5 further suggest that parameter a may depend on RH_∞ itself, with larger values of a corresponding to drier environments. In particular, we found that a can be best approximated as a function of $(1-RH_\infty)^2$. Hence, data shown on figure 5a for $\lambda = 0.5$ can be well fitted by the following relationship:

$$\eta = 0.47 - 0.0079\,(1-RH_\infty)^2\, b_m'^{-1.7}. \tag{45}$$

Best fit values for a, b and η_0 are summarized in table 2 for both $\lambda = 0.5$ and $\lambda = 2$. Replacing equation 45 in 43 yields a new entrainment parameterization that can be used directly in convective plume models.

4. Comparison with existing entrainment/detrainment parameterizations

We have already mentioned that equation 26 reduces to $\varepsilon \propto r_m^{-1}$ when top-hat velocity and buoyancy profiles are assumed across the plume. Such a simple relationship, confirmed by water tank experiments from which a coefficient of proportionality of 0.2 has been deduced, has been previously employed in 1D convective cloud models, for example by (Simpson and Wiggert 1969). It is however only valid in the case of entrainment in a pure jet, that is in an updraft forced mechanically without internal source of momentum from buoyancy.

Recognizing the limitations of such a crude model, many authors have developed more elaborate entrainment rate parameterizations accounting for in-plume and environmental conditions, or buoyancy reversal at cloud edge due to evaporative cooling. In the following, similarities between equation **??** and various successful entrainment models discussed in the literature are highlighted to stress the universality of the proposed model.

a. The buoyancy sorting model

The buoyancy sorting concept introduced by (Raymond and Blyth 1986) relies on a rather simple principle. Mixing between moist and dry environmental air produces a range of mixtures (stochastic by nature) which, after evaporation of the liquid fraction until saturation, may become negatively buoyant. It is then assumed that all negatively buoyant parcels detrain while positively buoyant mixtures are entrained. In other words, all mixtures for which $\chi > \chi_{cr}$ detrain, and the net entrainment/detrainment rate can be characterized by the local χ_{cr} value only. Practical implementations have been proposed in (Kain and Fritsch 1990) for a stochastic version, or (Bretherton et al. 2004) for a deterministic representation of mixing.

In section 3, we followed (Raymond and Blyth 1986; Bretherton et al. 2004) and described mixing between environmental and cloudy air assuming that all mixtures possible are equally likely to be found (i.e. all χ values are associated with the same probabilities of occurrence). By calculating buoyancy for each mixture after evaporation and integrating over all possible values of χ, we essentially followed a procedure equivalent to the buoyancy sorting method. We have however introduced a crucial difference by considering a Gaussian velocity profile across the plume. The importance of considering a Gaussian updraft velocity is illustrated in figure 6, which also provides a graphical interpretation for equation 26.

While all negatively buoyant mixtures are supposed to detrain in the buoyancy sorting approach, the presented model determines whether a mixed parcel will detrain or not based on the balance between buoyancy and inertia. If buoyancy reversal occurs far enough from the plume center, the low updraft velocities there will quickly become negative and detrainment occurs. However, if buoyancy is found to be negative closer to the plume center, updraft velocities may be strong enough for the mixture to keep its positive momentum and entrainment of dry air results. As such,

equation 26 can be seen as an improvement over the deterministic buoyancy sorting model from (Bretherton et al. 2004), generally known to detrain too much (Bretherton et al. 2004; de Rooy et al. 2013), as it includes a physically motivated way to limit detrainment by considering updraft velocities inside the plume and the mixing layer.

b. Buoyancy dependent models

By neglecting the first term on the right hand side of **??**, i.e. if one assumes that the contribution from the plume's dynamics to entrainment dominates over the geometrical term $\propto r_m^{-1}$ (i.e. if the updraft core is wide enough and strongly forced, as expected for example in deep convective clouds), a simple relationship directly proportional to $b_c'/\rho_\infty w_c^2$ is found, with a constant of proportionality equal to η.

A similar formulation has been proposed by (Gregory 2001) who suggested a constant of proportionality of $1/12$. Later, based on LES results of shallow convective clouds analyzed from an entraining plume perspective, (de Rooy et al. 2013), (de Rooy and Siebesma 2010) and (Del Genio and Wu 2010) found good agreement between their model data and (Gregory 2001) for $\eta = 0.45$, $\eta = 0.31$ and $\eta \approx 0.4$ (below the freezing level) respectively. These values appear to agree well with the limit value of 0.47 found for relatively thin mixing layers and in the absence of evaporative cooling, $\chi_{cr} = 1$. Note that (Del Genio and Wu 2010) concluded that the model proposed by (Gregory 2001) constitutes a viable option for parameterizing entrainment in operational models.

c. Dependency on the critical mixing fraction χ_{cr}

Although we have primarily expressed ε as a function of the plume's buoyancy, it was shown that a strong relationship between fractional entrainment rates and χ_{cr} also exists (see figure 4). A similar conclusion has already been drawn from several cloud resolving model simulations

(de Rooy and Siebesma 2007; Böing et al. 2012), which provides some support for parameterizing ε as a function of χ_{cr}.

Starting from relation 44, and reevaluating η as a function of χ_{cr}, we find $\varepsilon \propto \left(\eta_0 - c\chi_{cr}^{-d}\right) \frac{Ri}{r_m}$, with c and d both positive, and Ri held constant. This relationship is somewhat similar to the formulations proposed by (Böing et al. 2012) based on cloud resolving model simulations of deep convection, or the deterministic buoyancy sorting model of (Bretherton et al. 2004), who however found reversed signs compared to the above proposition (a, b and η_0 are then < 0). Although quantitatively different, these various parameterizations may result in similar behaviors for ε as a function of environmental humidity and temperature anomaly (see figure 7).

d. A direct comparison

To summarize, figure 7 compares the behavior of several common entrainment parameterizations and equation 45 (i.e. with $\lambda = 0.5$) for various environmental relative humidities, and two values of the temperature difference between the cloud and its environment. In both cases, the vertical velocity is set to 1 m/s, the pressure to 700 hPa and the cloud liquid mixing ratio to 2 g/kg.

Except for the parameterization from (Gregory 2001), all models tested predict an increase of ε with environmental relative humidity. In the low temperature anomaly case, only the model based directly on the buoyancy sorting concept (Bretherton et al. 2004) is consistent with our equation 45, allowing detrainment at low relative humidity, in addition to a steep decrease of ε with RH_∞. In the high temperature anomaly case, all models predict positive entrainment rates, with (Gregory 2001) giving the best quantitative agreement with 45 (i.e. relatively large ε). Although not evident at first sight, the present comparison tends to confirm that relation 45 results in a similar qualitative description of entrainment as the buoyancy sorting concept.

It should be emphasized here that the present discussion constitutes a very preliminary attempt at comparing our formulation with existing parameterizations. All parameterizations compared have indeed been taken out of context (that is completely decoupled from a parent convection scheme and its host model providing realistic meteorological conditions), and only a narrow range of environmental conditions have been tested. Generalizing these conclusions would require performing systematic comparisons in a more realistic context with the proposed entrainment formulation fully coupled to a comprehensive convection parameterization.

5. Conclusion

Starting with the Reynolds averaged Euler equations describing a steady-state turbulent axisymmetric plume, a number of integral equations describing the plume's ascent in a sheared environment are derived using as few simplifications as possible. In particular, general shapes of the updraft velocity and buoyancy profiles across the plume are maintained, resulting in the introduction of several shape parameters in the final equations. The general flux equations are then used to derive: (1) a closure for the fractional rate of lateral mixing (including both entrainment and detrainment) by enforcing consistency between the kinetic energy and vertical momentum integral equations, and (2) a set of primitive equations for the plume's mean properties that can readily be used in classical 1D models.

In the absence of environmental shear, the fractional entrainment rate is expressed as a function of the plume's convective Richardson number quantifying the ratio between buoyancy and vertical inertia. When considering specific updraft velocity and buoyancy profiles across the plume, namely Gaussian and linear profiles respectively, very different entrainment formulations and behaviors are obtained compared to the usual top-hat approximation. In particular, environmental air entrained into the plume is shown to affect the updraft through evaporative cooling, especially if

the mixture of environmental and cloudy air results in negatively buoyant air parcels. The fact that negatively buoyant mixtures may detrain from the plume is consistent with the buoyancy sorting concept, although in the present case detrainment only occurs if the original parcel's momentum (determined by the Gaussian profile) is not strong enough to maintain its ascent.

The impact of evaporative cooling on the entrainment process is quantified by a multiplicative factor shown to correlate strongly with the plume's average buoyancy and, to a lesser extent, with environmental relative humidity and the liquid water mixing ratio. By systematically varying the properties of the plume and its environment, this dependency can be characterized more precisely and takes the form of a hyperbolic function (negative power law) of the plume's buoyancy. As a whole, the fractional mixing rate is therefore found to be a strong function of the buoyancy itself, in such a way that a less buoyant plume is more likely to detrain, especially in a drier environment. The new entrainment formulation, combining equations **??** and 44 with appropriate parameters, can be directly used in any 1D plume model. In general, the dependence of entrainment on the plume's buoyancy and environmental humidity is supported by many recent cloud resolving model studies of shallow and deep convective clouds reported in the literature.

Several important assumptions had to be made for the equations to remain tractable and to arrive at these results. To start with, the plume was assumed to be in steady state and perfectly axisymmetric around its axis. Pressure gradient forces were treated in a simple way through the inclusion of a simple virtual mass parameter, thus neglecting many important dynamical interactions. All shape parameters as well as the velocity and buoyancy radial distributions were assumed to remain constant during the plume's ascent (full self-similarity indicating that turbulence is fully developed and the normalized plume geometry does not change). The updraft velocity profiles were given a Gaussian shape, while the buoyancy profiles were assumed to evolve linearly within a mixing layer of a given thickness, the latter being left undefined. All these assumptions and

limitations should be addressed in more detail for an improved characterization of lateral mixing at cloud/plume edge. For example, LES of convective (deep and shallow) clouds could be used to better constrain the radial distribution of many relevant quantities across the cloud as well as the precise shape and geometrical scales of the cloud edge mixing layer. More generally, LES should be used to assess the validity of the various relationships suggested here under a wide range of atmospheric conditions.

Acknowledgments. Funding for this research was provided by the Natural Environment Research Council (NERC) as part of project NE/N013727/1 entitled 'Using LES to characterize and parameterize the convective cloud field'. The authors would like to thank Steef Böing and two anonymous reviewers for their comments and suggestions that helped improve this manuscript.

References

Arakawa, A., and W. Schubert, 1974: Interaction of a cumulus cloud ensemble with the large-scale environment, part i. *J. Atmos. Sci.*, **31**, 674–701.

Bechtold, P., M. Köhler, T. Jung, F. Doblas-Reyes, M. Leutbecher, M. Rodwell, F. Vitart, and G. Balsamo, 2008: Advances in simulating atmospheric variability with the ecmwf model: from synoptic to decadal time-scales. *Q. J. R. Meteorol. Soc.*, **134**, 1337–1351.

Böing, S., A. Siebesma, J. Korpershoek, and H. Jonker, 2012: Detrainment in deep convection. *Geophys. Res. Lett.*, **39**, L20 816.

Bretherton, C., J. McCaa, and H. Grenier, 2004: A new parameterization for shallow cumulus convection and its application to marine subtropical cloud-topped boundary layers. part i: description and 1d results. *Mon. Wea. Rev.*, **132**, 864–882.

Chiang, H.-C., and B. Sill, 1985: Entrainment models and their application to jets in a turbulent cross flow. *Atmos. Env.*, **19**, 1425–1438.

Dawe, J., and P. Austin, 2011: Interpolation of les cloud surface for use in direct calculations of entrainment and detrainment. *Mon. Wea. Rev.*, **139**, 444–456.

Dawe, J., and P. Austin, 2013: Direct entrainment and detrainment rate distributions of individual shallow cumulus clouds in an les. *Atmos. Chem. Phys.*, **13**, 7795–7811.

de Roode, S., A. Siebesma, H. Jonker, and Y. de Voogd, 2012: Parameterization of the vertical velocity equation for shallow cumulus clouds. *Mon. Wea. Rev.*, **140**, 2424–2436.

de Rooy, W., and A. Siebesma, 2007: A simple parameterization for detrainment in shallow cumulus. *Mon. Wea. Rev.*, **136**, 560–576.

de Rooy, W., and A. Siebesma, 2010: Analytical expressions for entrainment and detrainment in cumulus convection. *Q. J. R. Meteorol. Soc.*, **136**, 1216–1227.

de Rooy, W., and Coauthors, 2013: Entrainment and detrainment in cumulus convection: an overview. *Q. J. R. Meteorol. Soc.*, **139**, 1–19.

Del Genio, A., 2012: Representing the sensitivity of convective cloud systems to tropospheric humidity in general circulation models. *Surv. Geophys.*, **33**, 637–656.

Del Genio, A., and J. Wu, 2010: The role of entrainment in the diurnal cycle of continental convection. *J. Clim.*, **23**, 2722–2738.

Fox, D., 1970: Forced plume in a stratified fluid. *J. Geophys. Res.*, **75**, 6818–6835.

Gregory, D., 2001: Estimation of entrainment rate in simple models of convective clouds. *Q. J. R. Meteorol. Soc.*, **127**, 53–72.

679 Hoult, D., J. Fay, and L. Forney, 1969: A theory of plume rise compared with field observations.
680 *J. Air Pollut. Control Ass.*, **19**, 585–590.

681 Kain, J., and J. Fritsch, 1990: A one-dimensional entraining/detraining plume model and its ap-
682 plication in convective parameterization. *J. Atmos. Sci.*, **47**, 2784–2802.

683 Kaminski, E., S. Tait, and G. Carazzo, 2005: Turbulent entrainment in jets with arbitrary buoyancy.
684 *J. Fluid. Mech.*, **526**, 361–376.

685 Klocke, D., R. Pincus, and J. Quaas, 2011: On constraining estimates of climate sensitivity with
686 present-day observations through model weighting. *Q. J. R. Meteorol. Soc.*, **127**, 53–72.

687 Korolev, A., A. Khain, M. Pinsky, and J. French, 2016: Theoretical study of mixing in liquid
688 clouds - part i: classical concepts. *Atmos. Chem. Phys.*, **16**, 9235–9254.

689 List, E., and J. Imberger, 1973: Turbulent entrainment in buoyant jets and plumes. *J. Hydraulic*
690 *Div. Proc. ASCE*, **99**, 1461–1474.

691 Morrison, H., 2016: Impacts of updraft size and dimensionality on the perturbation pressure and
692 vertical velocity in cumulus convection. part i: Simple, generalized analytic solutions. *J. Atmos.*
693 *Sci.*, **73**, 1441–1454.

694 Morton, B., G. Taylor, and J. Turner, 1956: Turbulent gravitational convection from maintained
695 and instantaneous sources. *Proc. R. Soc. Lond. A*, **234**, 1–23.

696 Ooyama, K., 1971: A theory on parameterization of cumulus convection. *J. Meteor. Soc. Japan*,
697 **49**, 744–756.

698 Raymond, D., and A. Blyth, 1986: A stochastic mixing model for non-precipitating cumulus
699 clouds. *J. Atmos. Sci.*, **43**, 2708–2718.

Romps, D., 2010: A direct measurement of entrainment. *J. Atmos. Sci.*, **67**, 1908–1927.

Romps, D., and A. Charn, 2015: Sticky thermals: Evidence for a dominant balance between buoyancy and drag in cloud updrafts. *J. Atmos. Sci.*, **72**, 2890–2901.

Romps, D., and Z. Kuang, 2010: Nature versus nurture in shallow convection. *J. Atmos. Sci.*, **67**, 1655–1666.

Rotunno, R., and J. Klemp, 1982: The influence of the shear induced pressure gradient on thunderstorm motion. *Mon. Wea. Rev.*, **110**, 136–151.

Schatzmann, M., 1979: An integral model of plume rise. *Atmos. Env.*, **13**, 721–731.

Simpson, J., and V. Wiggert, 1969: Models of precipitating cumulus towers. *Mon. Wea. Rev.*, **97**, 471.

Stirling, A., and R. Stratton, 2012: Entrainment processes in the diurnal cycle of deep convection over land. *Q. J. R. Meteorol. Soc.*, **138**, 1135–1149.

Turner, J., 1986: Turbulent entrainment: the development of the entrainment assumption, and its application to geophysical flows. *J. Fluid. Mech.*, **173**, 431–471.

van Reeuwijk, M., and J. Craske, 2015: Energy-consistent entrainment relations for jets and plumes. *J. Fluid. Mech.*, **782**, 333–355.

LIST OF TABLES

Symbol	description
a, b	Tunable parameters in entrainment parameterization
b'	Buoyancy
B	Integral buoyancy
c_{pa}, c_{pv}	Heat capacities at constant pressure for dry air and water vapor
e, f, g	Radial distributions for the density, tangential velocity and scalar respectively
e_s	Saturation vapor pressure
F	Integral buoyancy flux
$I_{1,\ldots,7}, J_{1,4,5}$	Shape integrals and modified shape integrals
k	Total kinetic energy inside the plume
K	Integral kinetic energy flux
L_v	Latent heat of vaporization
g	Gravitational acceleration
M	Integral mass flux
N_∞^2	Buoyancy frequency
p	Pressure
P	Integral momentum flux
$q_{v,l,s}$	Water vapor, liquid and saturated vapor mixing ratios
Q_φ	Integral scalar source/sink
$\{r, s\}$	Normal and tangential coordinates in the plume's local reference frame
RH	Relative humidity
R_a, R_v	Specific gas constants for dry air and water vapor
S	Integral scalar flux
T	Temperature
u, w	Horizontal and vertical velocity components in the original coordinate system
U_∞	Crossflow horizontal velocity
v_s, v_r	Normal and tangential velocity components in the local coordinate system
V_e	Entrainment velocity
x, z	Horizontal and vertical coordinates in the Cartesian frame

α_1, α_2	Entrainment parameters (dimensionless)
β	Momentum related shape parameter
ε	Fractional entrainment rate
ζ	Energy consistent shape parameter
γ	Kinetic energy related shape parameter
κ	Scalar related shape parameter
ξ	Plume angle related shape parameter
σ	Buoyancy related shape parameter
θ	Potential temperature
ρ	Density
χ	Mixing fraction
η	Factor in entrainment parameterization
λ	Mixing layer thickness
ϖ_φ	Scalar sources/sinks
cr	Subscript: critical values (corresponding to a neutrally buoyant mixture)
m	Subscript: top-hat equivalent quantities inside the plume
∞	Subscript: quantities defined in the far field environment
$'$	Excess quantities within the plume (with respect to the environment)
$''$	Turbulent perturbation quantities
$\tilde{}$	Density weighted Reynolds averages
$\bar{}$	Regular Reynolds averages
$\langle . \rangle_0$, $\langle . \rangle$	Superscript: mixture properties before and after evaporation

TABLE 1. List of symbols.

Mixing layer	η_0	a	b
$\lambda = 2$	0.82	-0.0089	-2
$\lambda = 0.5$	0.47	-0.0079	-1.7

TABLE 2. Optimal parameterizations for the η coefficient given by equation 44, for thin and thick mixing layers.

LIST OF FIGURES

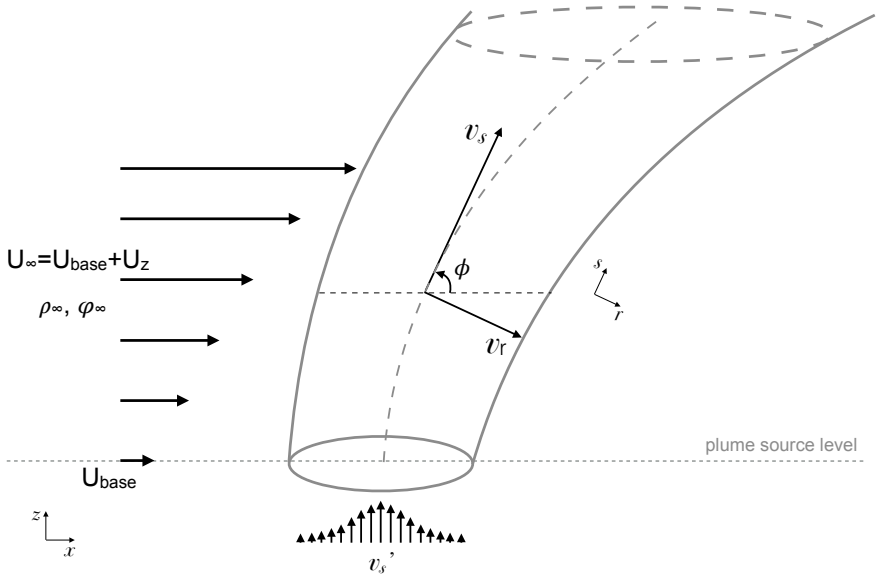

753 FIG. 1. Schematic representation of the plume's axisymmetric geometry. Variables with subscript ∞ denote
754 environmental conditions. v_s and v_r represent the flow velocities in the plume based coordinate system $\{r,s\}$. v_s'
755 is the excess $s-$velocity inside the plume defined in section b and here characterized by an approximate Gaussian
756 radial profile (shown at the base).

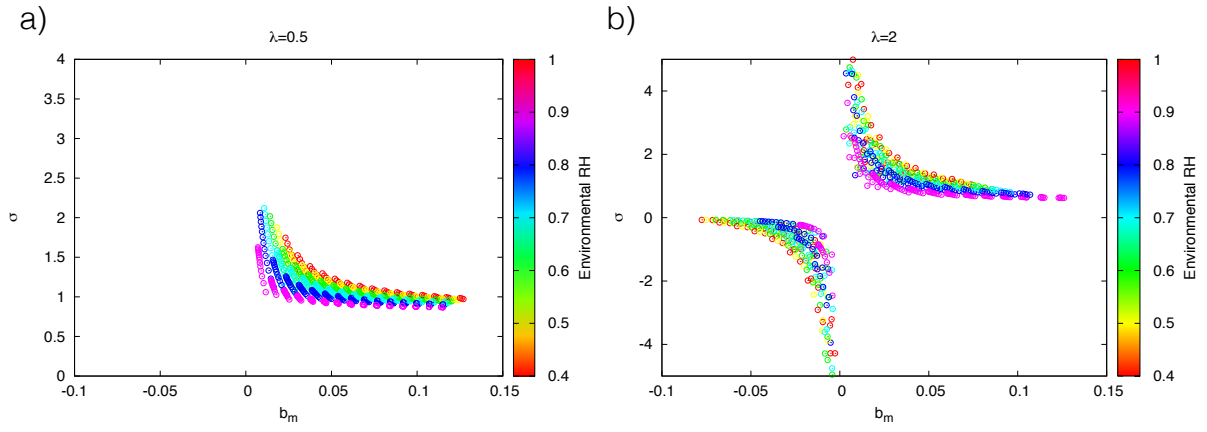

FIG. 2. Parameter σ as a function of the critical mixing fraction χ_{cr} for two values of the mixing layer thickness and colored by environmental relative humidity: a) $\lambda = 2$, b) $\lambda = 0.5$.

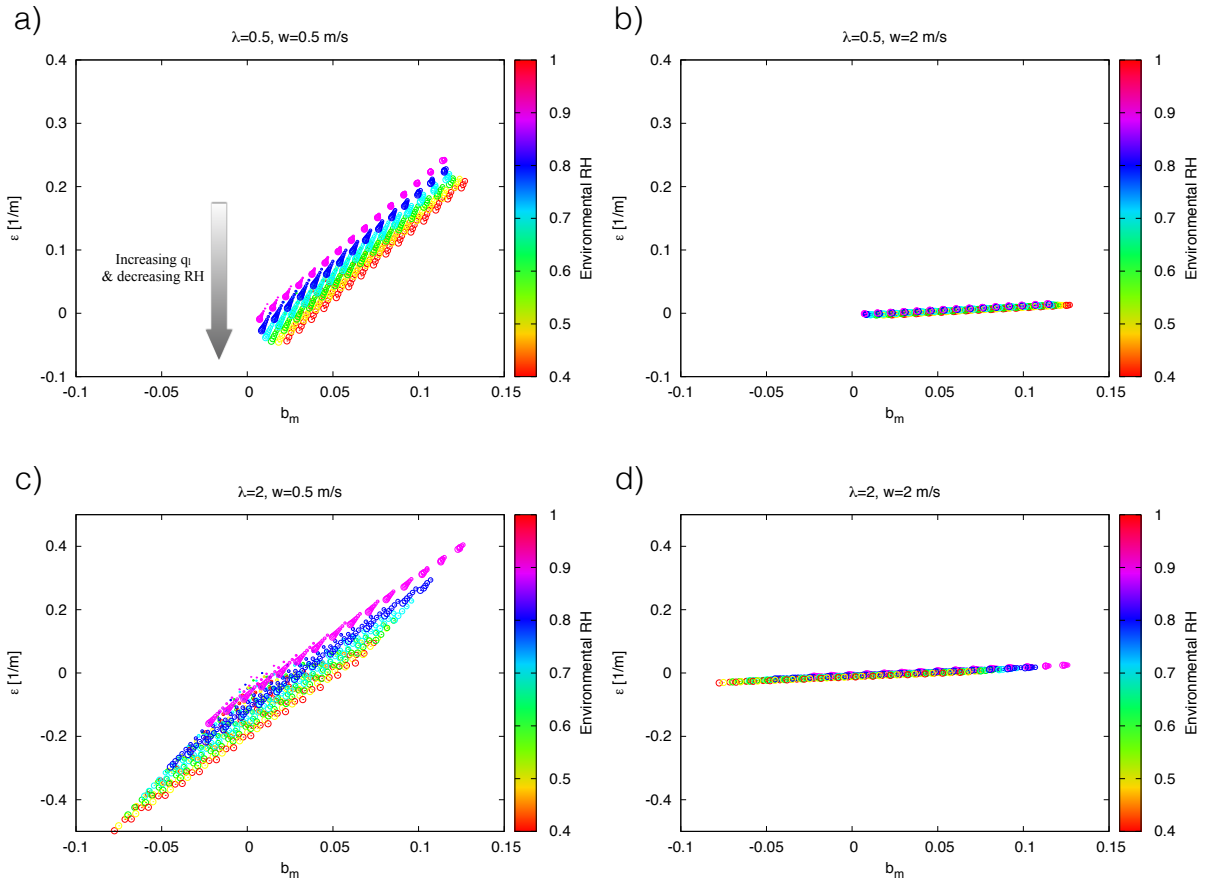

FIG. 3. Fractional entrainment rate as a function of the plume's top-hat buoyancy: a) and b) $\lambda = 0.5$, b) and d) $\lambda = 2$ (note the different vertical axes). Symbols are colored according to the environmental relative humidity and scaled by the liquid water mixing ratio (varying between 0.1 g/kg for the smallest symbols and 2 g/kg for the largest). The grey arrow in the top left panel denotes the direction for decreasing environmental RH.

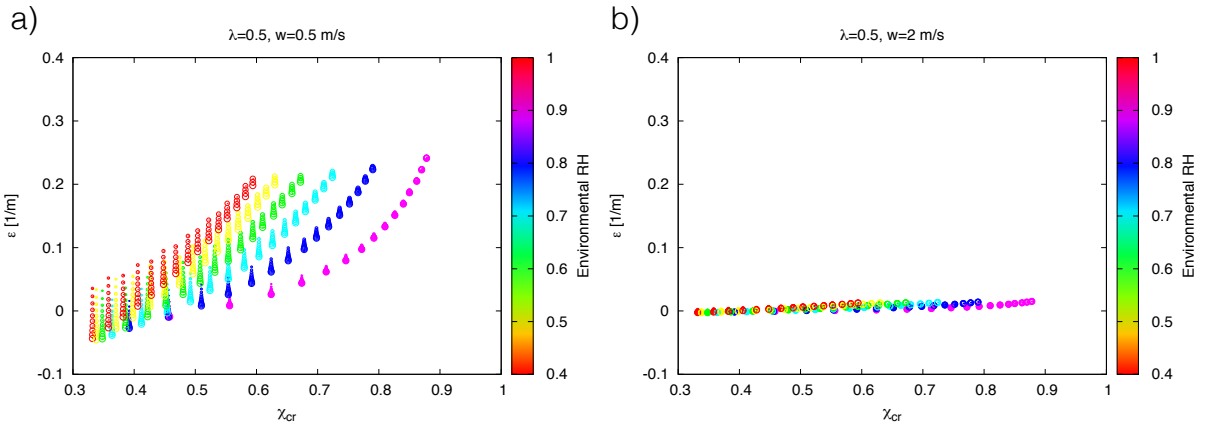

763 FIG. 4. Same as figure 3 but representing the fractional entrainment rate as a function of the critical mixing
764 fraction and for $\lambda = 0.5$ only.

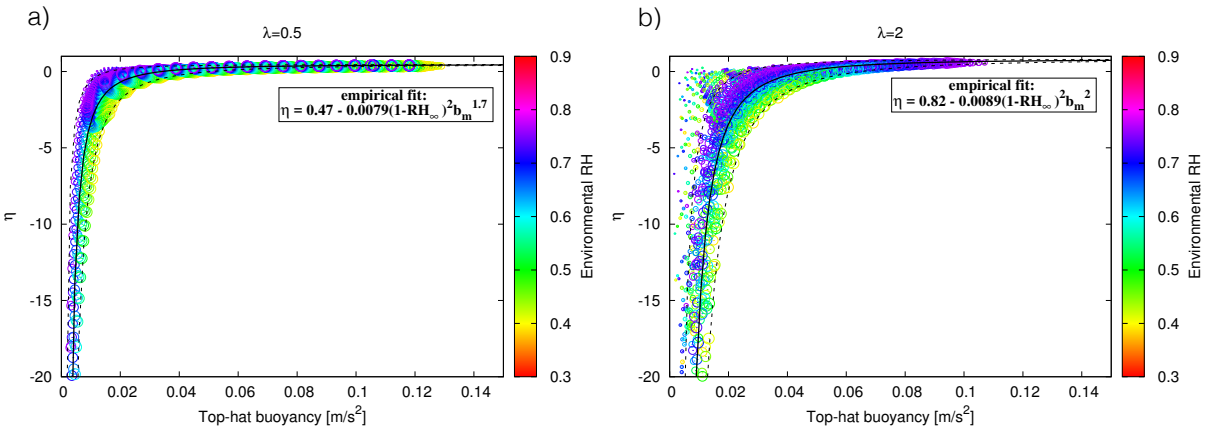

765 FIG. 5. Coefficient η as a function of plume buoyancy for: a) $\lambda = 0.5$, and b) $\lambda = 2$. Black lines represent
766 best fit estimates based on equation 44 for extreme (dashed lines) and mean (solid lines) values of RH_∞. The
767 corresponding empirical fits are given in the inserts.

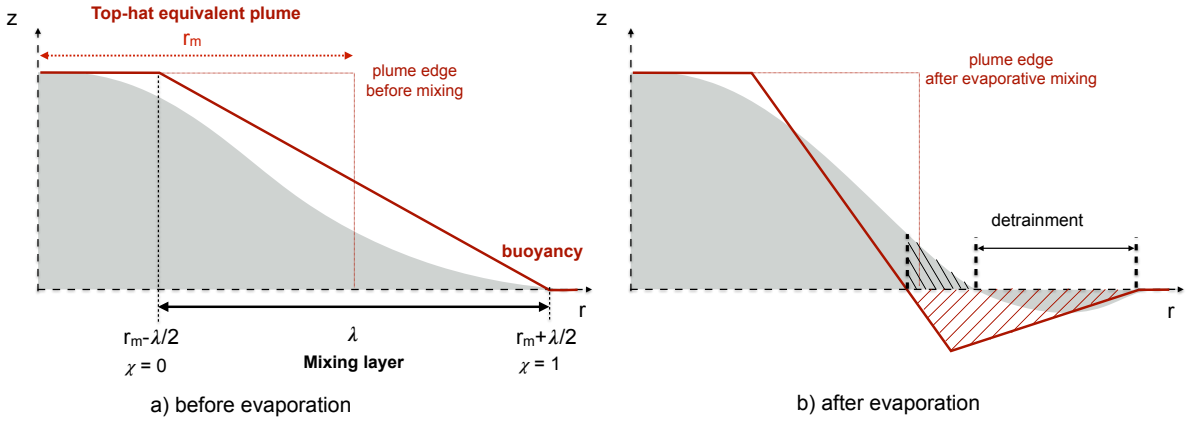

768 FIG. 6. Schematic representation of entrainment/detrainment as modeled by equation 26. a) Radial plume
769 structure after mixing but before evaporation. b) Radial plume structure after evaporation. Thick red lines
770 represent radial buoyancy profiles, shaded areas illustrate the (Gaussian) updraft velocity distribution, and thin
771 thin red lines indicate the position of the top-hat equivalent plume (before and after mixing and evaporation)
772 in such a way that the surface area below these lines should correspond to the surface area of the grey shaded
773 region. In b), the detrainment zone is marked by a thick arrow, the red hatched area corresponds to the region
774 where buoyancy becomes negative after evaporation (detrained in a buoyancy sorting model), the black hatched
775 area corresponds to the region where buoyancy is negative but the updraft velocity remains positive.

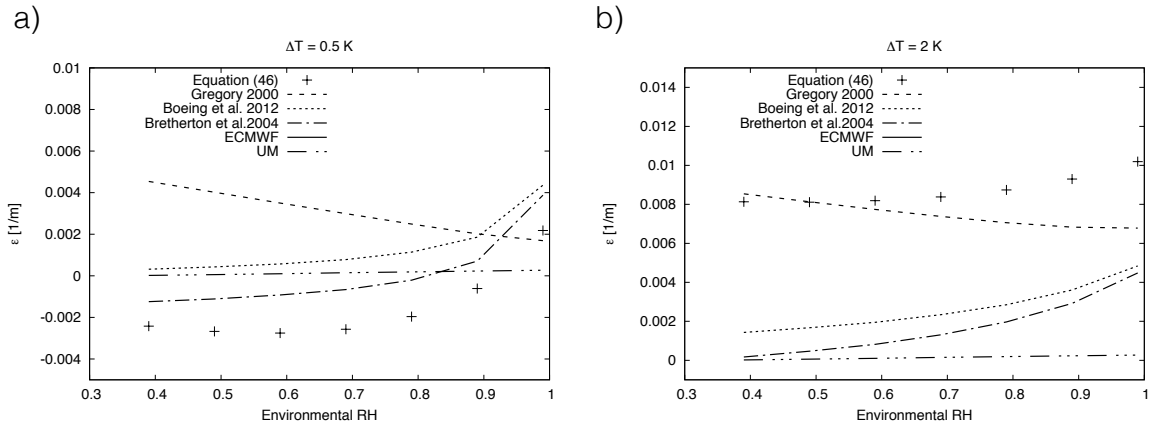

FIG. 7. Entrainment rate predicted by equation 45 as a function of environmental relative humidity for temperature anomalies of a) $\Delta T = 0.5\ K$ and b) $\Delta T = 2\ K$. Other commonly used parameterizations are reported here for comparison: these are taken from Gregory (Gregory 2001), Böing et al. (Böing et al. 2012), Bretherton et al. (Bretherton et al. 2004), Bechtold et al. (Bechtold et al. 2008) (ECMWF) and Stirling and Stratton (Stirling and Stratton 2012) (Unified Model, UM). q_l was fixed to $2\ g/kg$ in all cases.